Stochastic Linear Programming for Optimal Planning of Battery Storage Systems Under Unbalanced-uncertain Conditions

Reza Hemmati and Hasan Mehrjerdi

***Abstract*—Battery energy storage system (BESS) has already been studied to deal with uncertain parameters of the electrical systems such as loads and renewable energies. However, the BESS have not been properly studied under unbalanced operation of power grids. This paper aims to study the modelling and operation of BESS under unbalanced-uncertain conditions in the power grids. The proposed model manages the BESS to optimize energy cost, deal with load uncertainties, and settle the unbalanced loading at the same time. The three-phase unbalanced-uncertain loads are modelled and the BESSs are utilized to produce separate charging/discharging pattern on each phase to remove the unbalanced condition. The IEEE 69-bus grid is considered as case study. The load uncertainty is developed by Gaussian probability function and the stochastic programming is adopted to tackle the uncertainties. The model is formulated as mixed-integer linear programming and solved by GAMS/CPLEX. The results demonstrate that the model is able to deal with the unbalanced-uncertain conditions at the same time. The model also minimizes the operation cost and satisfies all security constraints of power grid.**

***Index Terms*—Battery energy storage system (BESS), single-phase storage planning, unbalanced loading, uncertainty.**

I. Introduction

ELECTRIC power systems and specifically electric distribution networkds often operate under unbalanced condition due to the installation of many single-phase loads as well as the unsymmetrical distribution of three-phase loads on the feeders [1]. The unbalanced currents of such loads flow through power grid lines and produce unbalanced voltage in the grid. As a result, the unbalanced loading condition creates a set of unbalanced voltages/currents in power grid, and decreases the power quality. The unbalanced voltages usually have undesirable impacts on power grid [2]. The unbalanced condition increases power losses in the grid and may deteriorate the operation of the protection relays [3], where the unbalanced voltage relay is applied to deal with such a problem. The unbalanced voltages also increase energy losses of the induction motors and decrease their efficiency and longevity [4]. The operation of the induction motors under unbalanced condition needs proper facilities [5].

The unbalanced condition is related to the concept of power quality, and several methods have been proposed to reduce the unbalanced level or remove the unbalanced condition. The voltage source inverters are the main technologies to deal with power quality issues. The proper control and operation of the inverters can successfully reduce the unsymmetrical loading level in power grid [6]. The active filters based on the different inverter topologies can successfully inject the desirable voltages/currents to the power grid and remove the unbalanced condition. In this regard, series, shunt, and combined active filters are widely utilized [7].

As stated, the voltage source inverters are one of the main technologies to cope with the unbalanced voltages in power grids [8]. The battery energy storage systems (BESSs) can also be considered as similar technologies. The BESSs are charged during off-peak time periods and discharged during on-peak time periods [9], [10]. The batteries produce DC voltage and they are connected to the AC grid by an interfacing inverter, which can be properly controlled to regulate active/reactive power, voltage, and frequency of power grid. The three-phase inverter between the battery and power grid can operate under unbalanced conditions and correct the unbalanced voltages/currents by injecting proper voltages on the three phases. It is also possible to apply three parallel single-phase inverters under the unbalanced condition [9]. These energy storage systems can deal with fluctuations of solar [10] and wind energies, and play a vital role in energy management [11], load leveling [12], peak cutting [13] and reliability improvement [14].

One of the abilities of BESS is to operate in unbalanced state [15]. The unbalanced operation of BESS has been investigated and confirmed. However, there are several knowledge gaps in the unbalanced operation of BESS that have not been addressed so far. The batteries can be controlled to provide different charging/discharging patterns on their phases. In other words, each phase can provide a separate charging/discharging pattern to deal with the unbalanced condition. This issue has not been addressed in the previous studies. As well, the unbalanced operation of BESS under uncertain condition has not been properly investigated. This paper

Manuscript received: May 14, 2019; accepted: August 26, 2019. Date of CrossCheck: August 26, 2019. Date of online publication: XX XX, XXXX.

R. Hemmati (corresponding author) is with the Department of Electrical Engineering, Kermanshah University of Technology, Kermanshah, Iran (e-mail: reza.hematti@gmail.com).

H. Mehrjerdi is with Qatar University, Doha, Qatar (e-mail: hasan.mehrjerdi@qu.edu.qa).

DOI: 10.35833/MPCE.2019.000324

bridges these gaps and presents a novel planning on BESS under unbalanced-uncertain condition at the same time. A different charging/discharging pattern is optimized for each phase of the battery system.

In the offered technique, BESSs are utilized in order to achieve various benefits including removing the unbalanced condition, smoothing the uncertainty, and improving energy management. In order to realize these objectives, the model is expressed as standard optimization programming and solved by general algebraic modeling system (GAMS). The programming finds the best level for power, capacity, location, and hourly operation of the batteries. The highlights of the proposed problem are summarized as follows:

1) The BESS are planned under the unbalanced loading condition. The loading on different phases of three-phase system is modeled as unbalanced. A charging/discharging pattern is optimized for each phase of battery storage system to cope with the unbalanced loading on the phases. The batteries under the unbalanced condition provide different charging/discharging pattern on each phase of the system.

2) The loading uncertainty is modeled by normal probability distribution function. The battery planning tackles the uncertainty and balances the loading at the same time.

3) The stochastic programming is applied to solve the problem with the uncertainty.

4) The objective function of the optimization programming is to minimize the energy cost, handle the uncertainty, and balance the unsymmetrical loading all together.

5) The plan determines optimal place, capacity, power, and charging/discharging regime of the batteries.

6) The problem models IEEE 69-bus feeder and it is solved by GAMS software.

7) A number of analyses and comparative studies show the practicality and proficiency of the introduced paradigm. It is demonstrated that the proposed technique can successfully balance the unsymmetrical loading, damp out the uncertainty, and minimize the cost of consumed energy.

BESS are connected to the network through the interfacing inverter as depicted in Fig. 1 [16], where P_a, P_b and P_c are the power of phases *a*, *b* and *c*, respectively; and P_{dc} is the power of DC section. The interfacing inverter can be efficiently controlled to manage the output power of the battery and schedule its operation. This structure can also be made by three single-phase inverters as depicted in Fig. 2, where P_{La}, P_{Lb} and P_{Lc} are the load power related to phases *a*, *b* and *c*, respectively; and P_{dca}, P_{dcb} and P_{dcc} are the DC power related to phases *a*, *b* and *c*, respectively. In both models, it is possible to share unbalanced loads on the three output phases of the inverter. The storage unit follows a similar charging/discharging pattern on all the three phases with the balanced loading. The inverter is also able to generate separate charging/discharging patterns on each phase under the unbalanced loading condition. The different charging/discharging power on each phase can effectively deal with the unbalanced loads installed next to the storage unit. Figure 2 shows that the charging/discharging power of the storage unit is added to the power of unbalanced load to make a balanced loading condition, i.e., $P_{La} \pm P_a = P_{Lb} \pm P_b = P_{Lc} \pm P_c$.

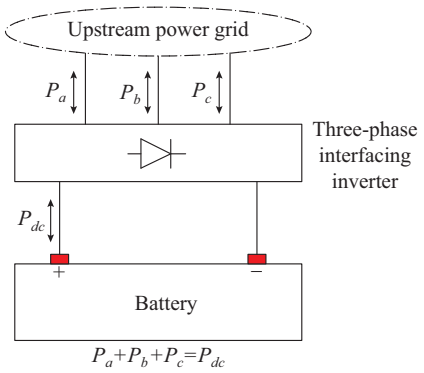

Fig. 1. Battery connected to power grid by three-phase interfacing inverter.

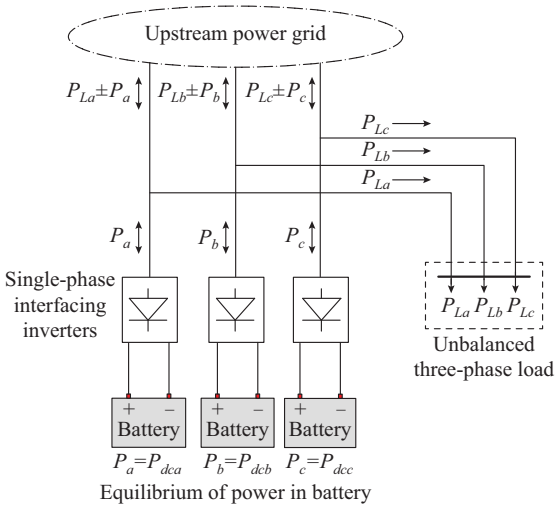

Fig. 2. Battery connected to power grid and unbalanced load.

II. Mathematical Modelling

A. Objective Function of Model

The objective function of the optimization programming is defined by (1). The first term of (1) shows the energy cost of the loads on all three phases. This term is multiplied by T_{pl} in order to elaborate the daily cost to the annual cost. The second term of (1) denotes the capital cost of inverter between the battery and the grid. This term is recognized as investment cost on the power of BESS. This cost is also defined per equivalent annual cost. The third term of (1) indicates the equivalent annual cost of BESS capacity and the last term is the annual operation cost of BESS.

$$\begin{cases} O_{fp} = Term_1 + Term_2 + Term_3 + Term_4 \\ Term_1 = T_{pl} \sum_{s\in S}\sum_{n\in N}\sum_{t\in T}\Big[\big(L_a^{s,n,t} + P_{ca}^{n,t} - P_{da}^{n,t} + L_b^{s,n,t} + P_{cb}^{n,t} \\ \qquad -P_{db}^{n,t} + L_c^{s,n,t} + P_{cc}^{n,t} - P_{dc}^{n,t}\big) F_e^t R_{sc}^s \Big] \\ Term_2 = F_b^p \dfrac{r(1+r)^y}{(1+r)^y - 1} \sum_{n\in N} P_{bn}^n \\ Term_3 = F_b^c \dfrac{r(1+r)^y}{(1+r)^y - 1} \sum_{n\in N} C_{bn}^n \\ Term_4 = F_b^{mo} T_{pl} \sum_{n\in N} C_{bn}^n \end{cases} \tag{1}$$

where s is the index for scenarios; S is the set of scenarios; n is the index of buses; N is the set of buses; t and T are the index and set of time intervals, respectively; $L_a^{s,n,t}$, $L_b^{s,n,t}$ and $L_c^{s,n,t}$ are the loads (p.u.) on phases a, b and c, respectively; $P_{ca}^{n,t}$, $P_{cb}^{n,t}$ and $P_{cc}^{n,t}$ are the charging power (p.u.) of storage unit on phases a, b and c, respectively; $P_{da}^{n,t}$, $P_{db}^{n,t}$ and $P_{dc}^{n,t}$ are the discharging power (p.u.) of storage unit on phases a, b and c, respectively; F_e^t is the expense of electrical energy ($/p.u.); R_{sc}^s is the probability of occurrence for scenarios; T_{pl} is the conversion factor; P_{bn}^n is the nominal power of the storage system (p.u.); F_b^p is the investment cost for the power of the battery ($/p.u.); C_{bn}^n is the nominal capacity of the storage unit (p.u.); F_b^c is the investment cost for the battery capacity ($/p.u.); F_b^{mo} is the daily operational cost of the battery ($/p.u.); y is the asset life-time (year); r is the discount rate (%); and O_{fp} is the objective function of the problem.

B. Operation of Phase a

The constraints on the operation of phase a of the interfacing inverter are given by (2)-(8). The constraints (2)-(4) confirm that the interfacing inverter can only operate on charging state or discharging state at each hour. The constraints (5) and (6) verify that the decision making binary variables can get only zero and one, and the constraints (7) and (8) introduce the allowed range of the variables.

$$B_{ca}^{n,t} + B_{da}^{n,t} \le 1 \quad \forall n \in N, \forall t \in T \tag{2}$$

$$P_{ca}^{n,t} \le B_{ca}^{n,t} \cdot BM \quad \forall n \in N, \forall t \in T \tag{3}$$

$$P_{da}^{n,t} \le B_{da}^{n,t} \cdot BM \quad \forall n \in N, \forall t \in T \tag{4}$$

$$B_{ca}^{n,t} \in \{0,1\} \quad \forall n \in N, \forall t \in T \tag{5}$$

$$B_{da}^{n,t} \in \{0,1\} \quad \forall n \in N, \forall t \in T \tag{6}$$

$$P_{ca}^{n,t} \ge 0 \quad \forall n \in N, \forall t \in T \tag{7}$$

$$P_{da}^{n,t} \ge 0 \quad \forall n \in N, \forall t \in T \tag{8}$$

where $B_{ca}^{n,t}$ is the binary variable indicating the charging state of phase a; $B_{da}^{n,t}$ is the binary variable indicating the discharging state of phase a; and BM is a big number equal to 1000.

C. Operation of Phase b

The similar constraints on the operation of phase b of the inverter are presented. These constraints are given through (9) to (15). The operational constraints in (9) to (11) verify that the inverter can only charge energy or discharge energy in each time interval. In other words, the inverter cannot operate on both the charging and discharging states at the same time. As well, the permitted range of the binary and positive variables are defined through (12)-(15).

$$B_{cb}^{n,t} + B_{db}^{n,t} \le 1 \quad \forall n \in N, \forall t \in T \tag{9}$$

$$P_{cb}^{n,t} \le B_{cb}^{n,t} \cdot BM \quad \forall n \in N, \forall t \in T \tag{10}$$

$$P_{db}^{n,t} \le B_{db}^{n,t} \cdot BM \quad \forall n \in N, \forall t \in T \tag{11}$$

$$B_{cb}^{n,t} \in \{0,1\} \quad \forall n \in N, \forall t \in T \tag{12}$$

$$B_{db}^{n,t} \in \{0,1\} \quad \forall n \in N, \forall t \in T \tag{13}$$

$$P_{cb}^{n,t} \ge 0 \quad \forall n \in N, \forall t \in T \tag{14}$$

$$P_{db}^{n,t} \ge 0 \quad \forall n \in N, \forall t \in T \tag{15}$$

where $B_{cb}^{n,t}$ is the binary variable indicating the charging state of phase b; and $B_{db}^{n,t}$ is the binary variable indicating the discharging state of phase b.

D. Operation of Phase c

The operation of phase c is modeled by (16) to (22). The constraints (16) to (18) demonstrate that the inverter cannot operate on both the charging and discharging states at the same time and (19) to (22) introduce the permitted range of the binary and positive variables.

$$B_{cc}^{n,t} + B_{dc}^{n,t} \le 1 \quad \forall n \in N, \forall t \in T \tag{16}$$

$$P_{cc}^{n,t} \le B_{cc}^{n,t} \cdot BM \quad \forall n \in N, \forall t \in T \tag{17}$$

$$P_{dc}^{n,t} \le B_{dc}^{n,t} \cdot BM \quad \forall n \in N, \forall t \in T \tag{18}$$

$$B_{cc}^{n,t} \in \{0,1\} \quad \forall n \in N, \forall t \in T \tag{19}$$

$$B_{dc}^{n,t} \in \{0,1\} \quad \forall n \in N, \forall t \in T \tag{20}$$

$$P_{cc}^{n,t} \ge 0 \quad \forall n \in N, \forall t \in T \tag{21}$$

$$P_{dc}^{n,t} \ge 0 \quad \forall n \in N, \forall t \in T \tag{22}$$

where $B_{cc}^{n,t}$ is the binary variable indicating the charging state of phase c; and $B_{dc}^{n,t}$ is the binary variable indicating the discharging state of phase c.

E. Modelling of Unbalanced Loads

The nominal power of the interfacing inverter is calculated by (23) and (24). It is clear that the charging and discharging power is less than or equal to the nominal power, and the nominal power is a positive variable as defined by (25).

$$P_{ca}^{n,t} + P_{cb}^{n,t} + P_{cc}^{n,t} \le P_{bn}^{n} \quad \forall n \in N, \forall t \in T \tag{23}$$

$$P_{da}^{n,t} + P_{db}^{n,t} + P_{dc}^{n,t} \le P_{bn}^{n} \quad \forall n \in N, \forall t \in T \tag{24}$$

$$P_{bn}^{n} \ge 0 \quad \forall n \in N \tag{25}$$

The constraints for removing the unbalanced loading condition are given in (26) and (27). These constraints confirm the equilibrium of net power (the generated power minus the consumed power) on all three phases. The total net power on phase a must be equal to the total net power on phases b and c in order to remove the unbalanced condition in power grid.

$$L_a^{s,n,t} + P_{ca}^{n,t} - P_{da}^{n,t} = L_b^{s,n,t} + P_{cb}^{n,t} - P_{db}^{n,t} \quad \forall s \in S, \forall n \in N, \forall t \in T \tag{26}$$

$$L_b^{s,n,t} + P_{cb}^{n,t} - P_{db}^{n,t} = L_c^{s,n,t} + P_{cc}^{n,t} - P_{dc}^{n,t} \quad \forall s \in S, \forall n \in N, \forall t \in T \tag{27}$$

F. Operation of Battery Storage Unit

The operation of battery storage unit is modeled through (28)-(35). The efficiency of the battery is given in (28). The energy stored inside the battery is modeled by (29) and (30). The constraints (31) and (32) verify that the initial energy and the stored energy are positive variables. The saved energy inside the BESS is limited by the nominal capacity of the battery as given by (33). The maximum permitted capacity

and power of the storage units are restricted by (34) and (35).

$$\eta_b = \frac{\sum_{t\in T}\left(P_{da}^{n,t}+P_{db}^{n,t}+P_{db}^{n,t}\right)}{\sum_{t\in T}\left(P_{ca}^{n,t}+P_{cb}^{n,t}+P_{cb}^{n,t}\right)} \quad \forall n\in N \tag{28}$$

$$E_b^{n,t}=E_b^{n,t-1}+\left(P_{ca}^{n,t}+P_{cb}^{n,t}+P_{cb}^{n,t}\right)- \left(P_{da}^{n,t}+P_{db}^{n,t}+P_{db}^{n,t}\right)/\eta_b \quad \forall n\in N,\forall t\in T,t\neq 1 \tag{29}$$

$$E_b^{n,t=1}=E_b^{n,0}+\left(P_{ca}^{n,t}+P_{cb}^{n,t}+P_{cb}^{n,t}\right)- \left(P_{da}^{n,t}+P_{db}^{n,t}+P_{db}^{n,t}\right)/\eta_b \quad \forall n\in N,\forall t=1 \tag{30}$$

$$E_b^{n,t}\geq 0 \quad \forall n\in N \tag{31}$$

$$E_b^{n,0}\geq 0 \tag{32}$$

$$E_b^{n,t}\leq C_{bn}^{n} \quad \forall n\in N,\forall t\in T \tag{33}$$

$$C_{bn}^{n}\leq C_{\max}^{n} \quad \forall n\in N \tag{34}$$

$$P_{bn}^{n}\leq P_{\max}^{n} \quad \forall n\in N \tag{35}$$

where η_b is the efficiency of battery unit; $C_{\max}^{n}$ is the maximum permitted capacity of storage unit (p. u.); $P_{\max}^{n}$ is the maximum permitted power of storage unit (p. u.); $E_b^{n,t}$ is the energy of battery storage unit (p.u.); and $E_b^{n,0}$ is the initial energy of battery storage unit (p.u.).

G. Network Modelling

The security constraints are given through (36)-(40). The transmitted power is computed by (36). The constraint (37) sets the reference voltage angle on the slack bus. The flow in each line is limited by (38) and (39). The balance of power on all buses for all three phases is achieved by (40).

$$F_l^{s,n,m,t}=Y^{n,m}\left(\theta^{s,n,t}-\theta^{s,m,t}\right) \quad \forall s\in S,n\in N,m\in N,t\in T \tag{36}$$

$$\theta^{s,n=1,t}=\theta_0 \quad \forall s\in S,\forall t\in T \tag{37}$$

$$F_l^{s,n,m,t}\leq Fl_{\max}^{n,m} \quad \forall s\in S,n\in N,m\in N,\forall t\in T \tag{38}$$

$$F_l^{s,n,m,t}\geq -Fl_{\max}^{n,m} \quad \forall s\in S,n\in N,m\in N,t\in T \tag{39}$$

$$L_a^{s,n,t}+P_{ca}^{n,t}-P_{da}^{n,t}+L_b^{s,n,t}+P_{cb}^{n,t}-P_{db}^{n,t}+L_c^{s,n,t}+P_{cc}^{n,t}-P_{dc}^{n,t} + \sum_{m\in N}F_l^{s,n,m,t}=0 \quad \forall s\in S,n\in N,\forall t\in T \tag{40}$$

where $F_l^{s,n,m,t}$ is the power in the line from bus n to m; $Fl_{\max}^{n,m}$ is the maximum power in the line from bus n to m (p.u.); m is the index of buses; $Y^{n,m}$ is the capacitance of the line (p. u.); $\theta^{s,n,t}$ is the voltage angle on bus n (radian); $\theta^{s,m,t}$ is the voltage angle on bus m (radian); and θ_0 is the voltage angle on swing bus (radian).

III. AC and DC Power Flow

In this paper, DC power flow is adopted to model the network. However, the DC power flow is not able to consider the voltage changes and limits. In order to overcome such an issue and present the real outputs, the proposed model is implemented in two stages as follows.

Stage 1: DC power flow is applied and the problem is expressed as a linear optimization programming. The linear programming is solved by GAMS and the achieved output is the global optimal solution.

Stage 2: The final plan (output of the optimization programming) is modelled on power grid, and AC power flow is run to evaluate the impacts of the plan on power grid. The voltage profile and the voltage limit on all buses are checked, evaluated, and confirmed.

As a result, the proposed model utilizes both AC and DC power flows to achieve the minimum simulation time, real and accurate model, and global optimal solution. The minimum and maximum permitted levels for voltage magnitude on all buses are 0.9 p.u. and 1.1 p.u., respectively.

IV. Illustrative Test Case

The IEEE 69-bus standard grid is simulated as the test case. This network is depicted in Fig. 3 and its data can be found in [17]. The grid is linked to the upstream grid through bus 1. Figure 4 shows 24-hour loading profile of the network and Fig. 5 represents the 24-hour three-level electricity price in the network [18]. The lithium-ion (Li-ion) battery is adopted. The battery expense for power is 250 $/kW, its expense for capacity is 230 $/kWh, and the maintenance expense is set on 230 $/kWh. The efficiency of BESS is 95% and the life-expectancy is 10 years. The maximum permitted capacity and power of the storage units are 1.0 p. u. and 0.2 p. u., respectively. The discount rate is 10%. Four loads are unbalanced as shown in Fig. 6.

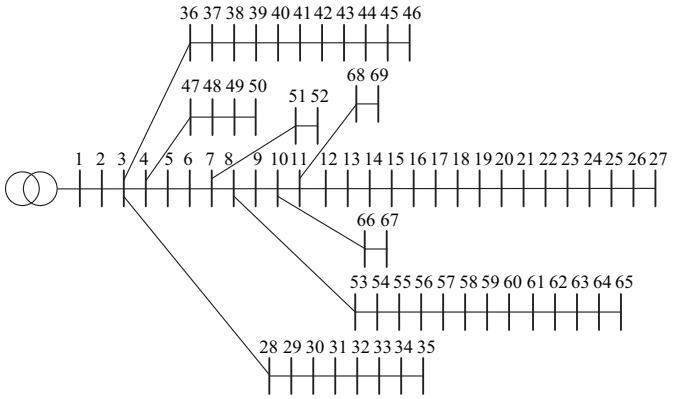

Fig. 3. Single line diagram of IEEE 69-bus network [17].

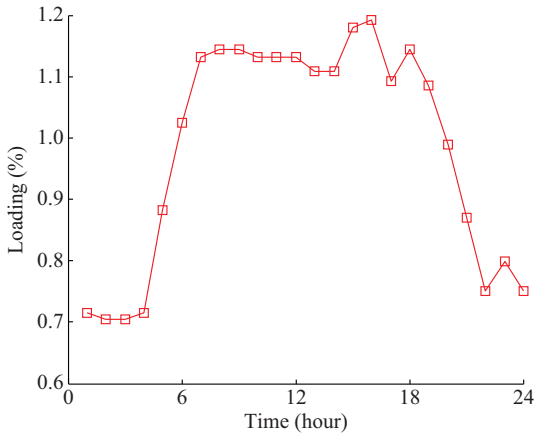

Fig. 4. Daily loading profile of network.

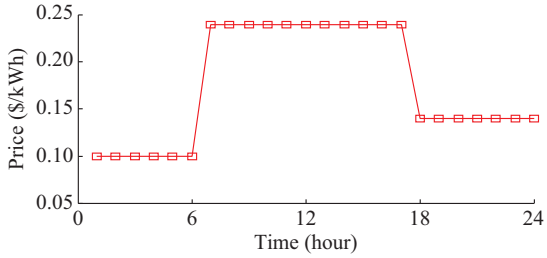

Fig. 5. Daily three-level electricity price in power grid.

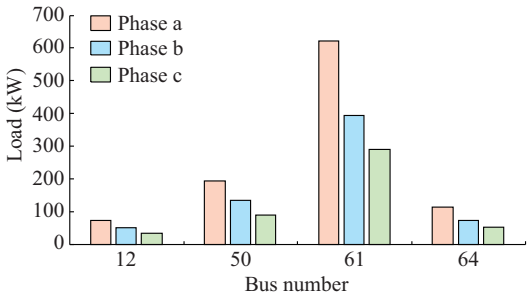

Fig. 6. Unbalanced loads installed in power grid.

The loading uncertainty is developed by Gaussian probability function [19]. It is possible to consider different probability distribution functions (PDFs) for uncertainty. However, the most common PDFs to model the load uncertainty is the Gaussian PDF [20]. This model has been widely adopted and applied in the literature [23], [24]. As well, it has been studied that all the available PDFs can be converted to an equivalent Gaussian PDF [21].

The uncertain parameters of the problem are modelled through stochastic programming. The scenario-generation and scenario-reduction techniques are applied to make the stochastic model [22]. The roulette wheel mechanism is applied to sample the scenarios from the distribution functions. The level and the probability of every scenario is calculated and recorded. After producing a large set of scenarios, the scenario-reduction technique is used to decrease the scenario number to the desired level. This study applies the backward scenario-reduction technique [22].

V. Simulation Results

The results under both the balanced and unbalanced loading conditions are presented. Tables I and II show the outputs of the planning under unbalanced and balanced loading conditions, respectively. It is clear that the unbalanced loading increases the planning cost by about $0.2 million per year. In addition, the total capacity and power installed with both the balanced and unbalanced loading are approximately similar. The total power installed with the balanced and unbalanced loadings are 0.82 p.u. and 0.83 p.u., respectively. The total installed capacities are also 4.86 p.u. and 4.93 p.u., respectively. As a result, the unbalanced loading condition does not need extra storage units to cope with the unsymmetrical loading condition, but it changes the location and capacities of the storage units in order to make the balanced condition. It is obvious that the unbalanced loading enforces the planning to install four storage units next to the unbalanced loads on buses 12, 50, 61, 64.

TABLE I
Output of Planning Under Unbalanced Loading Condition

Bus	Rated power (p.u.)	Rated capacity (p.u.)	Total planning cost (M$/year)
1	0.167	1.000	
4	0.167	1.000	
12	0.015	0.083	
16	0.170	1.000	6.1429
50	0.160	0.959	
61	0.123	0.722	
64	0.019	0.105	

TABLE II
Output of Planning Under Balanced Loading Condition

Bus	Rated power (p.u.)	Rated capacity (p.u.)	Total planning cost (M$/year)
1	0.167	1.000	
19	0.167	1.000	
20	0.054	0.272	5.9485
24	0.167	1.000	
26	0.167	1.000	
32	0.110	1.000	

The charging/discharging regime of the storage units installed with the balanced loading are depicted in Fig. 7. It is clear that they follow different patterns and often charges energy during low-cost or off-peak hours. Figure 8 shows the energy of three storage units installed with the balanced loading. The results demonstrate that the equilibrium of energy is obtained at all hours. Additionally, the energy at final stage is equal to the initial energy of the batteries. The energy losses in the battery and inverter are also demonstrated, where the total discharged energy from the storage units is less than the total charged energy into the storage units.

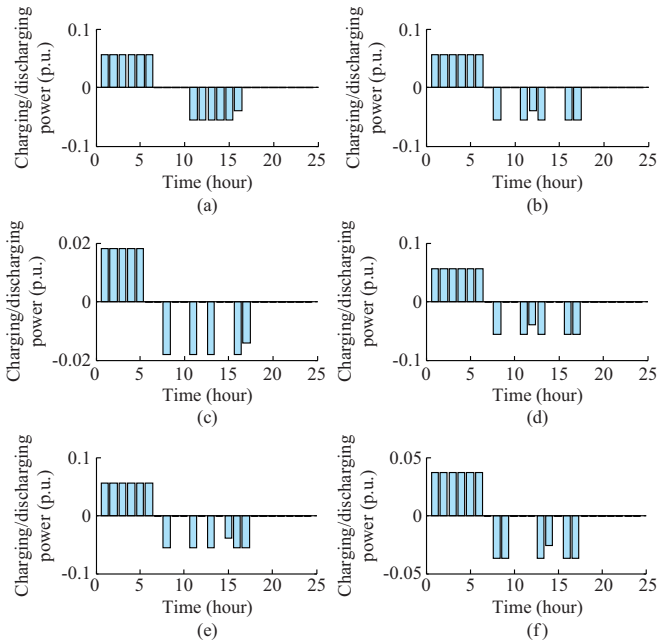

Fig. 7. Charging/discharging pattern of storage units installed with balanced loading. (a) Bus 1. (b) Bus 19. (c) Bus 20. (d) Bus 24. (e) Bus 26. (f) Bus 32.

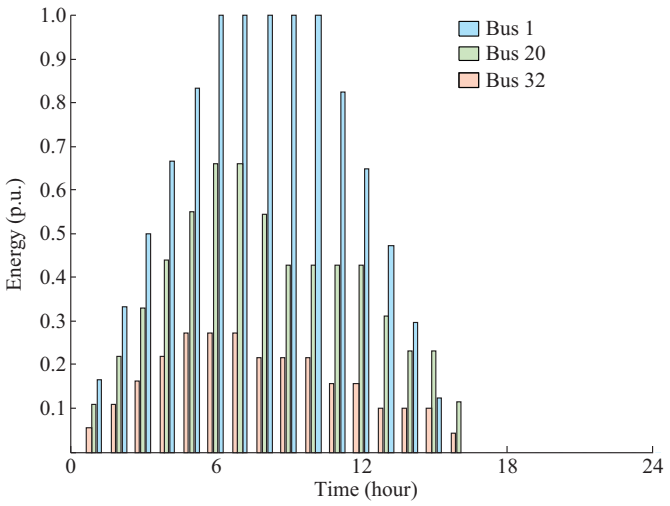

Fig. 8. Energy of storage units installed with balanced loading.

The charging/discharging pattern of the storage units installed with the unbalanced loading are listed in Table III. The pattern for the storage unit on bus 4 is not presented because it follows a similar pattern to bus 1. The storage units on bus 1 and bus 16 are installed next to the balanced loads, and the storage units on buses 12, 50, 61 and 64 are installed next to the unbalanced loads. It is clear that the storage units by the side of the balanced loads follow a similar charging/discharging pattern on all three phases. On the other hand, the storage units alongside the unbalanced loads follow different charging/discharging patterns on the three phases. For instance, the storage unit on bus 12 at hours 18-24 discharges the energy on phase *a*, and charges the energy on phase *c*. Phase *b* does not show significant charging/discharging operation. Such unsymmetrical operation of the battery storage units helps the power grid to overcome the unbalanced loading condition on bus 12. This has also been observed on the other buses suffering from the unbalanced loading.

In order to provide more details, Table IV lists the loading, charging/discharging power, and net load for bus 12. Table IV comprises three columns for each phase. The first column shows the loading on the phase at each hour and it is clear that the loading on the phases is unsymmetrical. The second column indicates the charging/discharging power at each hour, where the positive and negative values show the charging and discharging power, respectively. Eventually, the third column presents the total net load on each phase at each hour. The total net load is equal to the load plus the charging power minus the discharging power. The results show that the storage unit follows different charging/discharging patterns on three phases, but the total net loads on all three phases are equal and the network loading is symmetrical. As a result, the proposed methodology can successfully remove the unbalanced loading condition through optimal operation of battery storage units on different phases.

Figure 9 also depicts the energy of three storage units installed with the unbalanced loading. It is clear that the equilibrium of energy is verified at all hours. The stored energy to the batteries is more than the discharged energy for the sake of energy losses.

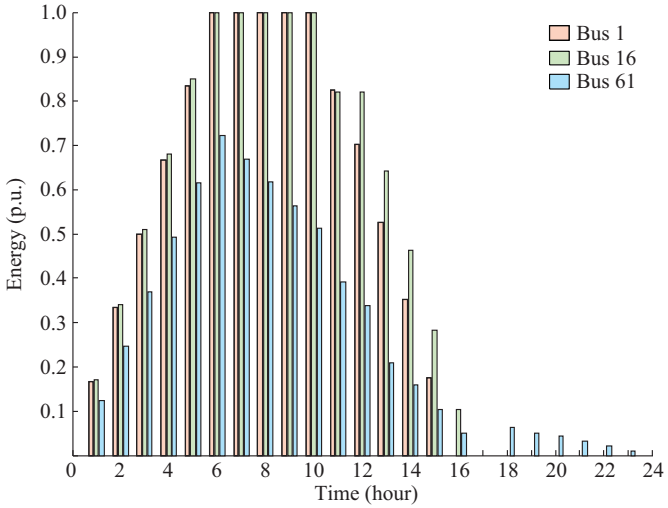

Fig. 9. Energy of storage units installed with unbalanced loading.

The total power received from the upstream grid is depicted in Fig. 10. It is clear that the network receives power from the upstream grid at most hours. However, at some hours such as hours 11, 13 and 14, the power grid sends the power to the upstream grid in order to reduce the energy cost of the network. This result confirms that the proposed methodology not only removes the unbalanced loading condition of the network, but also manages the storage units to reduce the operation cost of the network at the same time.

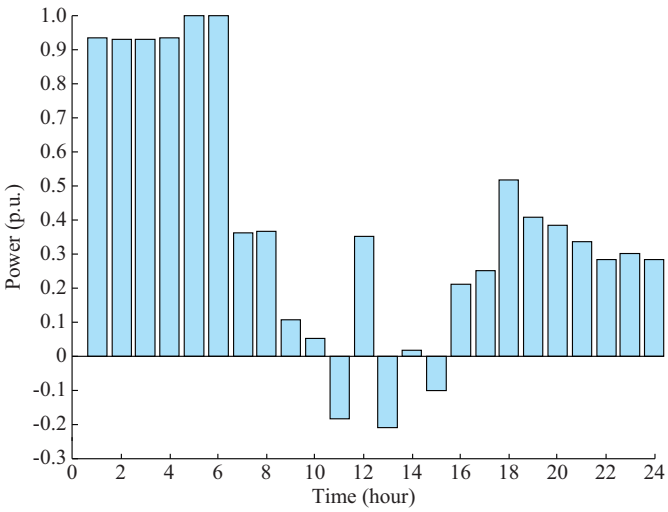

Fig. 10. Total power received from upstream grid.

Table V lists the planning cost under different unbalanced loading conditions. The planning cost increases together with the unbalanced loading. The most increment is observed when bus 61 is equipped with the unbalanced loading.

TABLE III
CHARGING/DISCHARGING POWER OF STORAGE UNITS INSTALLED WITH UNBALANCED LOADING

Time (hour)	Power on bus 1 (p.u.)			Power on bus 12 (p.u.)			Power on bus 50 (p.u.)		
	Phase a	Phase b	Phase c	Phase a	Phase b	Phase c	Phase a	Phase b	Phase c
1	0.05556	0.05556	0.05556	0.00367	0.00522	0.00643	0.04945	0.05358	0.05679
2	0.05556	0.05556	0.05556	0.00369	0.00522	0.00641	0.04951	0.05358	0.05673
3	0.05556	0.05556	0.05556	0.00369	0.00522	0.00641	0.04951	0.05358	0.05673
4	0.05556	0.05556	0.05556	0.00367	0.00522	0.00643	0.04945	0.05358	0.05679
5	0.05556	0.05556	0.05556	0.00333	0.00525	0.00674	0.04856	0.05365	0.05761
6	0.05556	0.05556	0.05556	0	0.00223	0.00397	0.04779	0.05371	0.05832
7	0	0	0	–0.00438	–0.00192	0	–0.01162	–0.00509	0
8	0	0	0	–0.00443	–0.00194	0	–0.01175	–0.00514	0
9	0	0	0	–0.00443	–0.00194	0	–0.05939	–0.05278	–0.04765
10	0	0	0	–0.00438	–0.00192	0	–0.05933	–0.05279	–0.04770
11	–0.05556	–0.05556	–0.05556	–0.00438	–0.00192	0	–0.05933	–0.05279	–0.04770
12	–0.03889	–0.03889	–0.03889	–0.00438	–0.00192	0	–0.01546	–0.00892	–0.00384
13	–0.05556	–0.05556	–0.05556	–0.00734	–0.00493	–0.00305	–0.05920	–0.05280	–0.04782
14	–0.05556	–0.05556	–0.05556	–0.00429	–0.00188	0	–0.01138	–0.00498	0
15	–0.05556	–0.05556	–0.05556	–0.00457	–0.00200	0	–0.05958	–0.05277	–0.04747
16	–0.05556	–0.05556	–0.05556	–0.00461	–0.00202	0	–0.01224	–0.00535	0
17	0	0	0	–0.00423	–0.00185	0	–0.01121	–0.00490	0
18	0	0	0	–0.00186	0.00063	0.00257	–0.00601	0.00059	0.00573
19	0	0	0	–0.00236	0	0.00184	–0.0057	0.00056	0.00544
20	0	0	0	–0.00215	0	0.00167	–0.00475	0.00097	0.00541
21	0	0	0	–0.00158	0.00032	0.00179	–0.00502	0	0.00391
22	0	0	0	–0.00163	0	0.00127	–0.00353	0.00081	0.00418
23	0	0	0	–0.00143	0.00030	0.00166	–0.00461	0	0.00359
24	0	0	0	–0.00163	0	0.00127	–0.00395	0.00039	0.00376
Time (hour)	Power on bus 16 (p.u.)			Power on bus 61 (p.u.)			Power on bus 64 (p.u.)		
	Phase a	Phase b	Phase c	Phase a	Phase b	Phase c	Phase a	Phase b	Phase c
1	0.057	0.057	0.057	0.028	0.044	0.051	0.004	0.007	0.008
2	0.050	0.050	0.050	0.028	0.044	0.051	0.004	0.007	0.008
3	0.057	0.057	0.057	0.028	0.044	0.051	0.004	0.007	0.008
4	0.057	0.057	0.057	0.028	0.044	0.051	0.004	0.007	0.008
5	0.057	0.057	0.057	0.025	0.045	0.054	0.003	0.007	0.009
6	0.050	0.050	0.050	0.016	0.040	0.050	0	0.004	0.006
7	0	0	0	–0.038	–0.012	0	–0.007	–0.002	0
8	0	0	0	–0.038	–0.012	0	–0.007	–0.002	0
9	0	0	0	–0.038	–0.012	0	–0.007	–0.002	0
10	0	0	0	–0.038	–0.012	0	–0.007	–0.002	0
11	–0.057	–0.057	–0.057	–0.060	–0.034	–0.022	–0.007	–0.002	0
12	0	0	0	–0.038	–0.012	0	–0.007	–0.002	0
13	–0.057	–0.057	–0.057	–0.062	–0.036	–0.025	–0.007	–0.002	0
14	–0.057	–0.057	–0.057	–0.037	–0.011	0	–0.007	–0.002	0
15	–0.057	–0.057	–0.057	–0.039	–0.012	0	–0.007	–0.002	0
16	–0.057	–0.057	–0.057	–0.040	–0.012	0	–0.007	–0.002	0
17	–0.033	–0.033	–0.033	–0.036	–0.011	0	–0.007	–0.002	0
18	0	0	0	0	0.026	0.038	–0.003	0.002	0.004
19	0	0	0	–0.025	0	0.011	–0.005	0	0.002
20	0	0	0	–0.020	0.002	0.013	–0.003	0.001	0.003
21	0	0	0	–0.020	0	0.009	–0.001	0.003	0.004
22	0	0	0	–0.017	0	0.008	–0.003	0	0.001
23	0	0	0	–0.018	0	0.008	–0.003	0	0.002
24	0	0	0	–0.017	0	0.008	–0.003	0	0.001

TABLE IV
LOADING, CHARGING/DISCHARGING POWER AND NET LOAD FOR BUS 12

Time (hour)	Phase a			Phase b			Phase c		
	Load (p.u.)	Charging/discharging power (p.u.)	Net load (p.u.)	Load (p.u.)	Charging/discharging power (p.u.)	Net load (p.u.)	Load (p.u.)	Charging/discharging power (p.u.)	Net load (p.u.)
1	0.00519	0.00367	0.00886	0.00363	0.00522	0.00886	0.00242	0.00643	0.00886
2	0.00510	0.00369	0.00879	0.00357	0.00522	0.00879	0.00238	0.00641	0.00879
3	0.00510	0.00369	0.00879	0.00357	0.00522	0.00879	0.00238	0.00641	0.00879
4	0.00519	0.00367	0.00886	0.00363	0.00522	0.00886	0.00242	0.00643	0.00886
5	0.00640	0.00333	0.00973	0.00448	0.00525	0.00973	0.00299	0.00674	0.00973
6	0.00744	0	0.00744	0.00521	0.00223	0.00744	0.00347	0.00397	0.00744
7	0.00821	–0.00440	0.00383	0.00575	–0.00192	0.00383	0.00383	0	0.00383
8	0.00830	–0.00440	0.00387	0.00581	–0.00194	0.00387	0.00387	0	0.00387
9	0.00830	–0.00440	0.00387	0.00581	–0.00194	0.00387	0.00387	0	0.00387
10	0.00821	–0.00440	0.00383	0.00575	–0.00192	0.00383	0.00383	0	0.00383
11	0.00821	–0.00440	0.00383	0.00575	–0.00192	0.00383	0.00383	0	0.00383
12	0.00821	–0.00440	0.00383	0.00575	–0.00192	0.00383	0.00383	0	0.00383
13	0.00804	–0.00730	0.00070	0.00563	–0.00493	0.00070	0.00375	–0.00305	0.00070
14	0.00804	–0.00430	0.00375	0.00563	–0.00188	0.00375	0.00375	0	0.00375
15	0.00856	–0.00460	0.00400	0.00599	–0.00200	0.00400	0.00400	0	0.00400
16	0.00865	–0.00460	0.00404	0.00605	–0.00202	0.00404	0.00404	0	0.00404
17	0.00792	–0.00420	0.00370	0.00555	–0.00185	0.00370	0.00370	0	0.00370
18	0.00830	–0.00190	0.00644	0.00581	0.00063	0.00644	0.00387	0.00257	0.00644
19	0.00787	–0.00240	0.00551	0.00551	0	0.00551	0.00367	0.00184	0.00551
20	0.00718	–0.00220	0.00502	0.00502	0	0.00502	0.00335	0.00167	0.00502
21	0.00631	–0.00160	0.00474	0.00442	0.00032	0.00474	0.00295	0.00179	0.00474
22	0.00545	–0.00160	0.00381	0.00381	0	0.00381	0.00254	0.00127	0.00381
23	0.00579	–0.00140	0.00436	0.00406	0.00030	0.00436	0.00270	0.00166	0.00436
24	0.00545	–0.00160	0.00381	0.00381	0	0.00381	0.00254	0.00127	0.00381

TABLE V
TOTAL PLANNING COST UNDER DIFFERENT UNBALANCED LOADING CONDITIONS

Bus with unbalanced loading	Planning cost (M$/year)	Increment of cost (%)
No unbalanced loading	5.9484	0.00
Bus 12	5.9680	0.33
Buses 12, 50	6.0200	0.87
Buses 12, 50, 61	6.1200	1.66
Buses 12, 50, 61, 64	6.1429	0.37

A. Stochastic Planning with Load Uncertainty

The proposed programming is a stochastic planning which can tackle the load uncertainty. In order to demonstrate the capability of the planning to deal with the uncertainty of the parameters, the loading of power grid is modeled by Gaussian probability function, and the results of stochastic planning are listed in Table VI. In order to provide better analysis, the results of the deterministic planning (i.e., the planning excluding uncertainty of the loads) are also presented. The results demonstrate that the stochastic planning increases the planning cost and installs different storage units on power grid to cope with the uncertainties. The total installed capacity of the stochastic plan is more than the deterministic one by 0.35 p.u., and such extra capacity is applied to handle the power grid uncertainties.

TABLE VI
RESULTS OF STOCHASTIC AND DETERMINISTIC PLANNING

Planning	Planning cost (M$/year)	Installed power for storage units (p.u.)	Installed capacity for storage units (p.u.)
Deterministic	6.020	Bus 1: 0.17; bus 4: 0.10; bus 12: 0.17; bus 14: 0.17; bus 16: 0.18	Bus 1: 1.0; bus 4: 0.63; bus 12: 1.0; bus 14: 1.0; bus 16: 1.0
Stochastic	5.968	Bus 1: 0.17; bus 3: 0.17; bus 12: 0.17; bus 20: 0.17; bus 23: 0.05; bus 41: 0.11	Bus 1: 1.0; bus 3: 1.0; bus 12: 1.0; bus 20: 1.0; bus 23: 0.28; bus 41: 0.66

Figure 11 shows the charging/discharging power on all three phases of the storage unit installed on bus 12 in the stochastic planning. It is clear that the storage unit presents separate charging/discharging power for each phase in order to make the loading balanced. This charging/discharging pattern follows three different purposes at the same time including removing the unbalanced loading condition, damping out the load uncertainty, and reducing the energy cost.

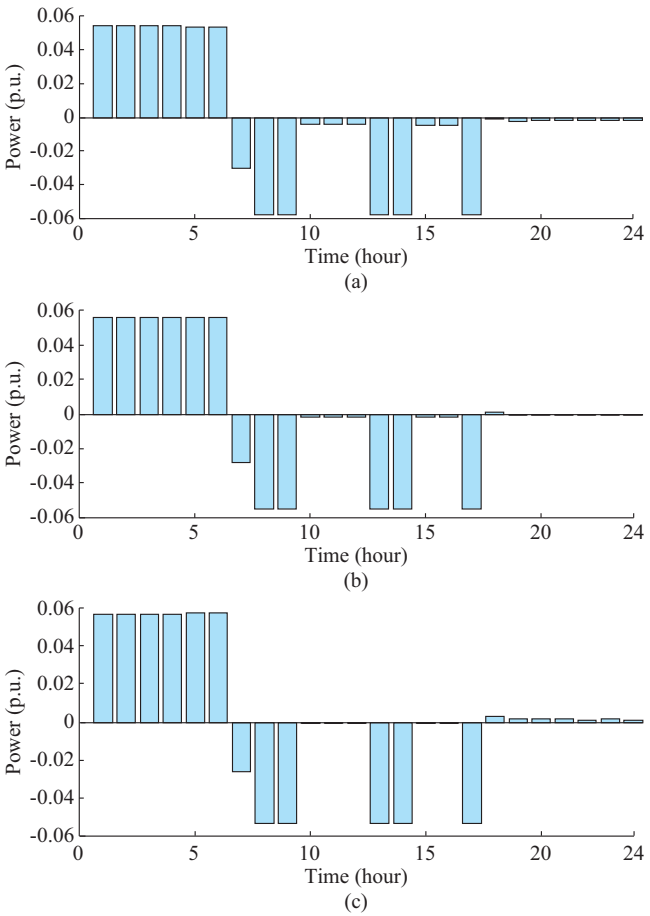

Fig. 11. Charging/discharging power on three phases of storage unit installed on bus 12. (a) Phase a. (b) Phase b. (c) Phase c.

B. Sensitivity Analysis

A sensitivity analysis is also carried out on the different parameters of the planning and the results are listed in Table VII. The first part of the table shows the sensitivity analysis on the uncertainty level. It is clear that increment of the uncertainty level increases the planning cost with a linear trend. The proposed model utilizes the BESS to deal with the uncertainty of power grid. When the uncertainty level is increased, the plan installs more energy storage units with larger capacities to deal with the uncertainty. The investment cost therefore increases, which result in more planning cost. In this regard, Table VI provides the useful information. In Table VI, the planning with uncertainty (stochastic planning) and the planning excluding uncertainty (deterministic planning) are compared. The results demonstrate that the stochastic planning installs more and larger storage systems to cope with uncertainties. The second part of the table shows a sensitivity analysis on the efficiency of storage unit. Reducing the efficiency by 10% can significantly increase the cost. But the reduction of efficiency behind 90% does not change the planning cost meaningfully. Another sensitivity analysis is conducted on the load level and the results are presented in the third part of the table.

TABLE VII
SENSITIVITY ANALYSIS ON DIFFERENT PLANNING PARAMETERS

Level	Sensitivity analysis	Planning cost (M$/year)
Uncertainty level	Uncertainty level of loading is 0%	6.020
	Uncertainty level of loading is 5%	6.040
	Uncertainty level of loading is 10%	6.057
	Uncertainty level of loading is 15%	6.071
Efficiency level	Efficiency is 100%	5.810
	Efficiency is 95%	6.020
	Efficiency is 90%	6.140
	Efficiency is 85%	6.144
	Efficiency is 80%	6.146
Loading level	Loading level is 0%	6.020
	Loading level is 10%	6.648
	Loading level is 20%	7.269
	Loading level is 30%	7.889

C. Results of Second Test Case

In order to verify the applicability of the proposed model, it is simulated on another test case. In this regard, the IEEE 33-bus test system is considered as second case study. The data of power grid can be found in [23]. The other data are assumed as the first test case. The results for this case are listed in Table VIII. It is clear that four energy storage systems are installed on power grid at different locations and their power and capacities are optimized by the planning. Such optimal sizing and siting properly deals with both the unbalanced-uncertain loadings in the network. It is demonstrated that the proposed model is applicable on different power grids.

TABLE VIII
OUTPUT OF PLANNING FOR THE SECOND TEST CASE

Bus number	Rated power (p.u.)	Rated capacity (p.u.)
5	0.13	1.00
15	0.05	0.40
21	0.10	0.90
31	0.15	1.00

VI. CONCLUSION

This paper presents an advanced planning on energy storage units to minimize the operation cost of power grid, handle the uncertainties, and remove the unbalanced loading condition simultaneously. The results verify that the unbalanced loading increases the planning cost by about $0.2 million per year. The total capacity and power of the storage units installed with both the balanced and unbalanced loadings are approximately equivalent. However, the unbalanced loading changes the location and charging/discharging patterns of the storage units to relive the unbalanced loading condition. The charging/discharging patterns indicate that the storage units under balanced loading condition follow a similar pattern on all three phases, while the units installed together with the unbalanced loads present different patterns

on each phase of the three-phase system. The equilibrium of energy at all hours, energy losses in the battery, and the equality of energy at initial and final hours are also verified by the simulations. The transferred power between the power grid and the upstream grid signifies that the power grid sends power to the upstream grid at hours 11, 13 and 14 in order to reduce the energy cost. The results show that the planning cost increases with the unbalanced loading. Moreover, the proposed planning is simulated with loading uncertainty and the results are compared to the deterministic planning. It is confirmed that the uncertainty increases the planning cost and installs more storage units on power grid.

REFERENCES

[1] J. Yaghoobi, M. Islam, and N. Mithulananthan, "Analytical approach to assess the loadability of unbalanced distribution grid with rooftop PV units," *Applied Energy*, vol. 211, pp. 358-367, Feb. 2018.

[2] J. L. Gonzalez-Cordoba, R. A. Osornio-Rios, D. Granados-Lieberman *et al*., "Correlation model between voltage unbalance and mechanical overload based on thermal effect at the induction motor stator," *IEEE Transactions on Energy Conversion*, vol. 32, no. 4, pp. 1602-1610, Dec. 2017.

[3] M. Sarkar, J. Jia, and G. Yang, "Distance relay performance in future converter dominated power systems," in *Proceedings of 2017 12th IEEE PowerTech Conference*, Manchester, UK, Jun. 2017, pp. 1-6.

[4] V. Huchche, N. R. Patne, and A. Junghare, "Computation of energy loss in an induction motor during unsymmetrical voltage sags–a graphical method," *IEEE Transactions on Industrial Informatics*, vol. 14, no. 5, pp. 2023-2030, May 2018.

[5] M. Al-Badri, P. Pillay, and P. Angers, "A novel in situ efficiency estimation algorithm for three-phase induction motors operating with distorted unbalanced voltages," *IEEE Transactions on Industry Applications*, vol. 53, no. 6, pp. 5338-5347, Nov.-Dec. 2017.

[6] E. Prieto-Araujo, A. Junyent-Ferré, G. Clariana-Colet *et al*., "Control of modular multilevel converters under singular unbalanced voltage conditions with equal positive and negative sequence components," *IEEE Transactions on Power Systems*, vol. 32, no. 3, pp. 2131-2141, May 2017.

[7] A. K. Panda and N. Patnaik, "Management of reactive power sharing & power quality improvement with SRF-PAC based UPQC under unbalanced source voltage condition," *International Journal of Electrical Power & Energy Systems*, vol. 84, pp. 182-194, Jan. 2017.

[8] H. M. Basri and S. Mekhilef, "Digital predictive current control of multi-level four-leg voltage-source inverter under balanced and unbalanced load conditions," *IET Electric Power Applications*, vol. 11, no. 8, pp. 1499-1508, Sept. 2017.

[9] P. Monica, M. Kowsalya, and P. Tejaswi, "Load sharing control of parallel operated single phase inverters," *Energy Procedia*, vol. 117, pp. 600-606, Jun. 2017.

[10] H. Mehrjerdi and E. Rakhshani, "Vehicle-to-grid technology for cost reduction and uncertainty management integrated with solar power," *Journal of Cleaner Production*, vol. 229, pp. 463-469, Aug. 2019.

[11] H. Mehrjerdi and R. Hemmati, "Modeling and optimal scheduling of battery energy storage systems in electric power distribution networks," *Journal of Cleaner Production*, vol. 234, pp. 810-821, Oct. 2019.

[12] H. Mehrjerdi, "Simultaneous load leveling and voltage profile improvement in distribution networks by optimal battery storage planning," *Energy*, vol. 181, pp. 916-926, Aug. 2019.

[13] H. Mehrjerdi, R. Hemmati, and E. Farrokhi, "Nonlinear stochastic modeling for optimal dispatch of distributed energy resources in active distribution grids including reactive power," *Simulation Modelling Practice and Theory*, vol. 94, pp. 1-13, Jul. 2019.

[14] H. Mehrjerdi and R. Hemmati, "Coordination of vehicle-to-home and renewable capacity resources for energy management in resilience and self-healing building," *Renewable Energy*, vol. 146, pp. 568-579, Feb. 2020.

[15] G. Carpinelli, F. Mottola, D. Proto *et al*., "Minimizing unbalances in low-voltage microgrids: optimal scheduling of distributed resources," *Applied Energy*, vol. 191, pp. 170-182, Apr. 2017.

[16] R. Hemmati and N. Azizi, "Optimal control strategy on battery storage systems for decoupled active-reactive power control and damping oscillations," *Journal of Energy Storage*, vol. 13, no. Supplement C, pp. 24-34, Oct. 2017.

[17] S. A. Taher and S. A. Afsari, "Optimal location and sizing of UPQC in distribution networks using differential evolution algorithm," *Mathematical Problems in Engineering*, vol. 2012, no. 1, pp. 1-20, Jun. 2012.

[18] R. Hemmati and H. Saboori, "Stochastic optimal battery storage sizing and scheduling in home energy management systems equipped with solar photovoltaic panels," *Energy and Buildings*, vol. 152, pp. 290-300, Oct. 2017.

[19] M. Bornapour, R. A. Hooshmand, A. Khodabakhshian *et al.*, "Optimal stochastic coordinated scheduling of proton exchange membrane fuel cell-combined heat and power, wind and photovoltaic units in micro grids considering hydrogen storage," *Applied Energy*, vol. 202, no. Supplement C, pp. 308-322, Sept. 2017.

[20] K. N. Hasan, R. Preece, and J. V. Milanović, "Existing approaches and trends in uncertainty modelling and probabilistic stability analysis of power systems with renewable generation," *Renewable and Sustainable Energy Reviews*, vol. 101, pp. 168-180, Mar. 2019.

[21] R. Hemmati, H. Saboori, and M. A. Jirdehi, "Stochastic planning and scheduling of energy storage systems for congestion management in electric power systems including renewable energy resources," *Energy*, vol. 133, pp. 380-387, Aug. 2019.

[22] M. Bornapour, R.-A. Hooshmand, A. Khodabakhshian *et al.*, "Optimal stochastic scheduling of CHP-PEMFC, WT, PV units and hydrogen storage in reconfigurable micro grids considering reliability enhancement," *Energy Conversion and Management*, vol. 150, pp. 725-741, Oct. 2017.

[23] F. Lezama, J. Soares, Z. Vale *et al*., "2017 IEEE competition on modern heuristic optimizers for smart grid operation: testbeds and results," *Swarm and Evolutionary Computation*, vol. 44, pp. 420-427, Feb. 2019.

Reza Hemmati received the Ph.D. degree in electrical engineering from Isfahan University, Isfahan, Iran, in 2013. Presently, he is assistant professor with the Department of Electrical Engineering, Kermanshah University of Technology, Kermanshah, Iran. His research interests include power systems planning, operation and control. He is among the top one percent of the world's most-cited researchers.

Hasan Mehrjerdi received the B.Sc. degree from the Ferdowsi University of Mashhad, Mashhad, Iran, the M.Sc. degree from Tarbiat Modares University, Tehran, Iran, and the Ph.D. degree from Québec University (École de Technologie Supérieure), Montréal, Canada, in 2010, all in electrical engineering. From 2011 to 2013, he was with the Power Systems and Mathematics Department, Research Institute of Hydro-Québec, Varennes, Canada. He was a senior power system researcher with Abengoa Research, Sevilla, Spain in 2014. In 2015, he joined Qatar University, Doha, Qatar, as an assistant professor. His current research interests include power system and protection studies, integration of renewable energy resources, and smart grid.